Electrocatalytic Reduction of Nitrate to Nitrous Oxide by a Copper-Modified Covalent Triazine Framework

Tatsuro Yoshioka,[†] Kazuyuki Iwase,[†] Shuji Nakanishi,[§] Kazuhito Hashimoto,[†,] and Kazuhide Kamiya[†,‡*]*

[†]Department of Applied Chemistry, The University of Tokyo, 7-3-1 Hongo, Bunkyo-ku, Tokyo 113-8656, Japan

[§]Research Center for Solar Energy Chemistry, Osaka University, 1-3 Machikaneyama, Toyonaka, Osaka 560-8531, Japan

[‡]Japan Science and Technology Agency (JST) PRESTO, 4-1-8 Honcho, Kawaguchi, Saitama 332-0012, Japan

KEYWORDS (Nitate reduction, Copper, Covalent triazine framework, Electrocatalyst).

Abstract

It was found that copper-modified covalent triazine frameworks (Cu-CTF) efficiently catalyze the electrochemical reduction of nitrate and promote N-N bond formation of nitrous oxide (N_2O), a key intermediate for N_2 formation (denitrification). A Cu-CTF electrode exhibited an onset potential of - 50 mV versus RHE for the electrochemical nitrate reduction reaction (NRR). The faradaic efficiency for N_2O formation by Cu-CTF reached 18% at - 200 mV versus RHE, whereas that for Cu metal was negligible. Based on density functional calculations for Cu-CTF, both solvated and surface-bound nitric oxide (NO) were generated by the NRR due to the moderate adsorption strength of Cu atoms for NO, a property that facilitated the effective dimerization of NO through an Eley–Rideal-type mechanism.

Introduction

The accumulation of nitrate ions in waste- and groundwater, which predominantly results from the poor drainage of wastewater and over-fertilization, has become a serious environmental issue.[1] It is reported that nitrate ions adversely affect the environment and human health.[2] For this reason, the development of simple and effective techniques for the remediation of nitrate-contaminated wastewaters is required.[3,4]

One promising approach for denitrification of water is the electrochemical reduction of nitrate. Electrochemical reduction methods are advantageous over biological treatments as they can operate under highly acidic conditions and in the presence of high nitrate concentrations. Electrochemical nitrate reduction reactions (NRR) in acidic solutions proceed through a stepwise mechanism and generate dinitrogen molecules (N_2) or ammonium ions (NH_4^+), as shown in Scheme 1.[5-11] Based on this reaction scheme, the reductive dimerization of NO to N_2O (bold line in Scheme 1) is a key step for the generation of harmless N_2, which is an ideal product of denitrification. Although some noble metal alloys, such as Pd-Cu[12] and Pt-Ni[13], showed the NRR activity in acidic solutions to give N_2 or N_2O as the main products, the N-N bond formation (N_2O or N_2 generation) is not promoted by non-noble metal based catalysts. For example, Taniguchi *et al.* showed that nickel or cobalt cyclam (cyclam = 1,4,8,11-tetraazacyclotetradecane) catalyzed the reduction of nitrate to hydroxylamine.[14] Furthermore, very recently, Shen *et al.* reported that ammonia and hydroxylamine were the main products of the NRR by a cobalt protoporphyrin immobilized on a graphite electrode.[15]

The N_2O generation that occurs during electrochemical NO reduction is facilitated through Eley–Rideal-type reactions, whereby solvated NO reacts with surface-bound NO.[11,16,17] Thus, the balance between the amount of NO released from electrode surfaces and the amount of

surface-bound NO critically affects the dimerization process. For this reason, optimal NRR electrocatalysts should have a moderate binding strength with NO. This requirement is highlighted by the fact that bulk platinum (Pt) electrodes, which interact strongly with NO, reduce surface-adsorbed NO to ammonia (path b in Scheme 1).[17-19] Conversely, on bulk copper (Cu) electrodes, which have the lowest overpotential for NRR among non-noble metals, generated NO molecules diffuse into the bulk electrolyte due to the weak binding between NO and bulk Cu (path d in Scheme 1).[7,20-22] Considering these literatures, the adsorption energy of NO on the surface which promotes the N-N bond formation should place between those on Cu and Pt. Therefore, the ability to precisely control the adsorption strength of NO molecules on electrocatalysts appears to be essential for accelerating the dimerization of NO to N_2O.

We recently developed a Cu-modified covalent triazine framework hybridized with carbon nanoparticles (Cu-CTF) and demonstrated that this system had the highest onset potential for the oxygen reduction reaction (ORR) among synthetic Cu-based ORR catalysts reported to date.[19] Extended X-ray absorption fine structure (EXAFS) measurements showed that Cu-CTF contains individually isolated Cu atoms within an unsaturated first coordination sphere. In this configuration, the Cu atoms have numerous accessible d-orbitals and low steric hindrance for adsorbates. The strong chemical interaction between Cu atoms and dioxygen due to this unsaturated coordination structure is essential for the high ORR activity of Cu-CTF and was confirmed by first principle calculations. Based on this property, Cu-CTF is expected to exhibit stronger binding to NO compared bulk Cu.

In the present paper, we demonstrated that single Cu sites in Cu-CTF selectively catalyze the reduction of nitrate to N_2O, which is the key intermediate for N_2 formation. In addition, our

findings also show that modulation of the adsorption energy of NO (ΔE_{NO}) is essential for the reductive dimerization of NO.

Experimental Section

Cu-CTF was prepared using the same method as described in our previous report.[23,24] Briefly, a mixture of $ZnCl_2$ (1.0 g, Wako), 2,6-dicyanopyridine (100 mg, Aldrich) and Ketjen Black EC600JD (100 mg, Lion Corp.) was heated in a vacuum-sealed glass tube at 400 °C for 40 h. The obtained CTF was washed with sequentially distilled water, tetrahydrofuran and 1 M HCl, and was then modified with Cu atoms using an impregnation method in a 1 mM $CuCl_2$ solution for 4 h at 60 °C. All electrochemical experiments were performed using a three-electrode system at room temperature. A platinum wire and Ag/AgCl/KCl (sat.) were used as the counter and reference electrodes, respectively. All potentials were calibrated with respect to a reversible hydrogen electrode (RHE). All solutions were deaerated by purging with argon prior to performing measurements. Nitrate reduction activities were evaluated in a 0.1 M $HClO_4$ electrolyte solution (pH 1). ^{15}N-labeled sodium nitrate ($Na^{15}NO_3$; Cambridge Isotope Laboratories, Inc.) was used as a nitrate source to exclude the possibility of detecting N-containing reaction products from the degradation of CTF. The catalyst ink was prepared by dispersing 4 mg Cu-CTF in 350 μL ethanol and 38 μL Nafion solution (5 wt%; Aldrich) using a homogenizer, and was added dropwise onto a glassy carbon electrode. The amount of loaded catalyst was controlled to be approximately 0.34 mg/cm^2. Cu metal electrodes (99.99%, BAS) as a reference were sequentially polished to a mirror finish with 1.00 and 0.05 μm aluminum suspensions.

Volatile products were analyzed by *in-situ* differential electrochemical mass spectrometry (DEMS) with a single-chamber electrochemical cell. The procedure for DEMS analysis is described in our previous paper.[25] DEMS signals of m/z = 2 (H_2), 30 ($^{15}N_2$ and fragment of $^{15}N_2O$), 31 (^{15}NO and fragment of $^{15}N_2O$) and 46 ($^{15}N_2O$) were examined. The fragmentation ratio of $^{15}N_2O$ was measured to obtain the mass signal corresponding to $^{15}N_2$ and ^{15}NO. In this work, the fragmentation ratio of $^{15}N_2O$ was determined as (m/z = 30) / (m/z = 46) = 0.18 and (m/z = 31) / (m/z = 46) = 0.45. The signals of $^{15}N_2$ and ^{15}NO were corrected for $^{15}N_2O$ fragmentation. A double-chamber electrochemical cell, in which the two chambers were separated by a Nafion membrane, was used for long-term electrolysis to estimate faradaic efficiencies (FE). Reaction products in the gas and liquid phases after long-term electrolysis were quantitatively analyzed by gas chromatograph mass spectrometry (GC-MS; GCMS-QP 2010 Plus, Shimadzu, Japan) and ion chromatography (IC; HIC-20A Super, Shimadzu, Japan), respectively.

Density functional theory (DFT) calculations for the adsorption energies of NO on Cu-CTF, Cu(111) and Pt(111) were performed using OpenMX code.[26,27] The generalized gradient approximation of the Perdew-Burke-Ernzerhof model (GGA-PBE) was applied, and a kinetic energy cutoff of 120 Ryd was selected. The p(3 × 3) cell of the metal surface was modeled as periodically repeated slabs consisting of three atomic layers. The bottom atomic layer was frozen and set to the estimated bulk parameters, and the remaining atomic layers were fully optimized. To simplify the DFT calculations, a slab consisting of a single Cu-CTF layer was used as the model structure of Cu-CTF with coordinatively unsaturated Cu atoms. The structural parameters are shown in Table S2. All slabs were separated by a vacuum spacing greater than 15 Å, as this

distance guarantees that no interactions would occur between the slabs. In this work, solvation, zero-point energy and entropic corrections were not applied (see, DFT results).

Results and discussion

Changes in current density (j) at different potentials (U) were examined for the Cu-CTF electrode in 0.1 M $HClO_4$ solutions with and without 0.1 M nitrate (Figure 1, curves 1 and 2, respectively). The NRR onset potential of the Cu-CTF catalyst was approximately -50 mV (vs. RHE), which was only approximately 100 mV smaller than that of a Cu metal electrode (Figure S1). In contrast, CTF (without Cu) generated almost no current, even in the presence of nitrate (Figure 1, curve 3). We also confirmed that Ketjen Black EC600JD exhibited no NRR activity (Figure S2). These findings, together with our previous work,[23] demonstrate that single Cu atoms in Cu-CTF serve as catalytic centers for the NRR. In addition, a single pair of redox peaks with a mid-point potential of 0.25 V vs RHE, which is 300 mV more positive than the NRR onset potential, was observed in the j versus U curve of Cu-CTF in the absence of nitrate (Figure S3). Thus, although the Cu^{2+} valence state is dominant in the as-prepared Cu-CTF as shown in our previous work[23], the Cu atoms with lower valence states likely reduce nitrate.

We next performed DEMS analysis to identify the volatile compounds produced during the cyclic voltammogram measurements. The mass signals assigned to H_2, $^{15}N_2$, ^{15}NO and $^{15}N_2O$, and the corresponding NRR currents for Cu metal electrodes and Cu-CTF are shown in Figure 2. In the case of the Cu metal electrode, only the mass signal corresponding to ^{15}NO increased in the potential region from 0.05 to -0.4 V, whereas the signals for $^{15}N_2O$ did not increase in any of the examined potential regions (Figure 2a). These results are consistent with a previous report examining the NRR for Cu metal electrode.[7] In contrast, for the DEMS analysis

of Cu-CTF showed that the mass signals of $^{15}N_2O$ was clearly increased with a smaller signal of ^{15}NO from the potential corresponding to the onset of the NRR current (Figure 2b), indicating that Cu-CTF reduced nitrate ions and promoted N-N bond formation of N_2O. Notably, the ratio of the N_2O signal to NRR current remained relatively constant in all examined potential regions, revealing that the FE of N_2O is not dependent on the applied potential. In the absence of nitrate, H_2 formation on Cu-CTF was observed from – 0.3 V (vs RHE). However, after the addition of 0.1 M nitrate to the electrolyte, the hydrogen evolution reaction (HER) did not occur at any examined potential region. These findings indicate that nitrate ions or NRR intermediates on the Cu sites suppress the adsorption of protons, and thus inhibit the HER, a property that is essentially consistent with Cu bulk metal and other reported molecular catalysts.[15,28]

Although the DEMS analysis confirmed that N_2O was formed in the Cu-CTF system through the NRR, these measurements do not provide quantitative information. In addition, non-volatile products, such as NO_2^- and NH_4^+, are not detectable by DEMS. Therefore, we used IC and GC-MS to quantitatively analyze NRR products in the liquid and gas phases, respectively, after long-term electrolysis. Figure S4 shows representative results of chronoamperometric measurements for Cu-CTF at – 0.2 V with 0.1 M nitrate. The cathodic current attributed to the NRR (approximately 1 mA/cm^2) was relatively stable for over 1 h. Notably, the reaction turnover number was at least 50, indicating that Cu-CTF is able to reduce nitrate catalytically (for the detail calculations see the Supporting Information). Figure 3 shows the FE for the NRR of Cu-CTF and Cu metal electrodes at – 0.2 V in 0.1 M and 1.0 M nitrate. The FE for N_2O production by Cu-CTF reached 18% and 76% in 0.1 M and 1 M nitrate, respectively, whereas the FE for N_2O of the Cu metal electrode was negligible. The concentration dependence of FE for N_2O is explained as follows. The high NRR current was obtained with increasing nitrate concentration

(ca. 6 mA/cm^2 in 1 M nitrate), resulting in the increase of the NO concentration in the near-surface region of Cu-CTF. Therefore, the dimerization of NO to N_2O efficiently proceeded.[12] In addition, the FE for N_2O showed little potential dependence between - 0.2 and - 0.6 V (Figure S5), a finding that is consistent with the DEMS results.

The main product of the NRR for both Cu-CTF and the Cu electrode was NH_4^+ (Figure 3b), and N_2, NO_2^- and hydrogen were not detected. As the DEMS measurements showed that solvated NO was present in bulk solution for both Cu-CTF and Cu bulk electrode, it is likely that NH_4^+ ions were predominantly formed via the further reduction of solvated NO (Scheme 1, path d), because NO is highly reactive and unstable (NO was not detectable by the GC-MS used in this study). However, it is also possible that a portion of the surface-bound NO was directly reduced to NH_4^+ (Scheme 1, path b).

Next, a detailed characterization of reactive centers for N_2O formation was conducted. We previously demonstrated using Fourier-transformed EXAFS (FT-EXAFS) spectra that Cu atoms in Cu-CTF are individually isolated and have an unsaturated first coordination sphere containing N atoms.[23] Here, curve fitting of FT-EXAFS spectra was conducted to further examine the structure of Cu-CTF (Figure S6).[29] The coordination structure of Cu-CTF was compared with that of 5,10,15,20-tetraphenyl-21H,23H-porphine copper(II) (Cu-TPP) because the coordination numbers (CN), elements and distances (R) of Cu-TPP are clearly defined. The estimated CN and R between Cu atoms and their nearest neighbors in Cu-CTF and Cu-TPP are listed in Table 1, and fitted curves for the FT-EXAFS spectra of these two molecules are shown in Figure S6. Although the Cu-N distances were similar between Cu-CTF and Cu-TPP, the CN of N atoms in the first coordination sphere of Cu-CTF (3.4) was smaller than that of Cu-TPP (4.0). These results indicate that the low-coordinated Cu atoms, which are generally unstable and

easily aggregate, are stabilized in the CTF framework through the formation of coordination bonds. Due to this configuration, the Cu sites in Cu-CTF may have open coordination sites and low steric hindrance for adsorbates.

Let us consider the mechanism of N-N bond formation by the single Cu sites of Cu-CTF. As mentioned in the Introduction, the moderate ΔE_{NO} of Cu-CTF may be essential for the reductive dimerization of NO to N_2O. To confirm this speculation, we calculated the ΔE_{NO} based on the DFT for Cu-CTF, Cu(111) and Pt(111) (Table 2). The calculated ΔE_{NO} of Pt(111) was 173 kJ/mol higher than that of Cu(111), a result that is consistent with the reported trend.[30-33] The ΔE_{NO} value for Cu-CTF was between that of Cu(111) and Pt(111), indicating that Cu-CTF has a more feasible binding strength for NO (see the Introduction). It should be noted here that although the calculated adsorption energies may differ from the actual values to some extent due to the lack of zero-point energy and entropic corrections, the trend among Cu, Pt and Cu-CTF is reliable as mentioned in the literatures.[34,35] In addition, as shown in the optimized structure of NO-bound Cu-CTF (Figure 4), it was confirmed that NO binds to an open coordination site of the Cu atoms in Cu-CTF, indicating that the open coordination site is the origin of the higher ΔE_{NO} for Cu-CTF compared to that of bulk Cu. Although, in this work, we focus on the unsaturated coordination structure, the oxidation state of Cu atoms during the NRR should affect the ΔE_{NO}. It has been reported that the Cu sites with lower valence states tend to bind to NO more strongly.[36] Unfortunately, though the CV results suggested that the valence state of Cu atoms is lower than 2+ during the NRR, the actual valency is still unclear. To provide more accurate NO adsorption strength on the Cu sites, computational calculations and *in situ* X-ray absorption near edge structure (XANES) to definite the oxidation state is now under investigation.

Based on the EXAFS results and DFT calculations, the mechanism of N_2O formation during the NRR by Cu-CTF can be explained as follows. The Cu sites in Cu-CTF appear to bind to NO more strongly than Cu bulk metal, likely because of the coordinatively unsaturated nature of the Cu centers in Cu-CTF. Therefore, a certain portion of NO remained adsorbed to the Cu sites in Cu-CTF, whereas most of the NO generated by the NRR on the Cu metal electrode freely diffuse into the bulk electrolyte. Thus, the solvated and surface-bound forms of NO react together on single Cu sites in Cu-CTF to form N_2O, as schematically illustrated in Figure 5. In Cu bulk metal, defective sites, such as kinks and steps, have a lower coordination number than that of terrace sites and thus may serve as reactive centers for N_2O formation. However, terrace sites, which are much more abundant than defect sites, effectively generate NO through the NRR (without N_2O formation), which likely explains why the FE of N_2O formation was negligible for Cu bulk metal.[21]

Meanwhile, nitrate adsorption strength is essential to facilitate the first reduction step of NRR (nitrate to nitrite)[34,35], although the main focus in this work is the NO adsorption for the N-N bond formation. Calle-Vallejo and Koper *et al.* clearly demonstrated that nitrate is a weakly-bound adsorbate even on Pt by using the DFT calculations.[35] As we assume that the tendency of adsorption strength of nitrate is similar to that of NO, the biding strength of nitrate on Cu-CTF should be considerably weaker than that on the optimal catalyst for nitrate reduction to nitrite. Further studies to calculate the nitrate adsorption strength and to design the catalyst with the suitable adsorption energy of not only NO and but also nitrate are in progress in our laboratory.

Conclusion

The present work demonstrated that Cu-CTF selectively catalyzes N_2O generation through the NRR. DFT calculations indicated that single Cu atoms of Cu-CTF strongly interact with NO due to their open coordination sites, resulting in enhanced NO dimerization through an Eley–Rideal-type mechanism. As the molecular structure of CTF can be specifically altered based on the type of building block that is selected, the selectivity of this material for nitrate reduction to N_2O can potentially be further increased by modulation of the Cu coordination structure and ΔE_{NO}. In addition, the addition of catalytic centers to reduce N_2O into optimized Cu-CTF can promote N_2 formation through the NRR. Taken together, the present findings demonstrate that single metal sites stabilized by CTF interact with reactants more strongly and selectively than the corresponding bulk metal. Thus, single-metal-atom-modified CTF electrocatalysts can potentially be designed and utilized for selective reactions, such as carbon dioxide reduction.

Table 1. Coordination number (CN), distance between the nearest neighbors (R), Debye−Waller factor (σ^2), and amplitude reduction factor (S_0^2) of Cu-TPP and Cu-CTF estimated from the Cu-K EXAFS analysis. When the CN of Cu-TPP was fixed at 4, S_0^2 was calculated to be 1.03, a value that was also used for Cu-CTF.[29]

	Bond type	CN	R (Å)	σ^2 ($\times10^{-3}$, Å)	S_0^2
Cu-TPP	Cu-N	4	1.99±0.02	4.1±4.0	1.03
Cu-CTF	Cu-N	3.4	2.01±0.01	7.2±2.1	1.03

Table 2. ΔE_{NO} of Cu(111), Cu-CTF and Pt(111).

Surface	ΔE_{NO} / kJ·mol^{-1}
Cu(111)	77.5
Cu-CTF	140.1
Pt(111)	250.6

ASSOCIATED CONTENT

Supporting Information. Curve fitting analysis of FT-EXAFS, CV for Cu metal electrode, chronoamperometry results, and product distributions at -0.6 and -0.4 V. This material is available free of charge via the Internet at http://pubs.acs.org.

AUTHOR INFORMATION

Corresponding Author

*(K.H.) E-mail: hashimoto@light.t.u-tokyo.ac.jp, (K.K.): kamiya@light.t.u-tokyo.ac.jp

Present Addresses

†If an author's address is different than the one given in the affiliation line, this information may be included here.

ACKNOWLEDGMENT

This research was supported by the PRESTO Program of the Japan Science and Technology Agency (JST). Synchrotron radiation experiments were performed using the BL01B1 Beam Line of SPring-8 with the approval of the Japan Synchrotron Radiation Research Institute (JASRI; Proposal Nos 2014B1252, 2015A1302 and 2015B1174). We thank Dr. T. Ina for providing technical support with the XAFS measurements at SPring-8.

ABBREVIATIONS

NRR, nitrate reduction reaction; CTF, covalent triazine framework; DEMS, differential electrochemical mass spectrometry;

REFERENCES

(1) Canfield, D. E.; Glazer, A. N.; Falkowski, P. G., The Evolution and Future of Earth's Nitrogen Cycle. *Science* **2010**, *330*, 192-196.

(2) Powlson, D. S.; Addisott, T. M.; Benjamin, N.; Cassman, K. G.; de Kok, T. M.; van Grinsven, H.; L'Hirondel, J. L.; Avery, A. A.; van Kessel, C., When Does Nitrate Become a Risk for Humans? *J. Environ. Qual.* **2008**, *37*, 291-295.

(3) Horold, S.; Vorlop, K. D.; Tacke, T.; Sell, M., Development of Catalysts for a Selective Nitrate and Nitrite Removal from Drinking-Water. *Catal. Today* **1993,** *17*, 21-30.

(4) Kapoor, A.; Viraraghavan, T. Nitrate Removal from Drinking Water - Review. *J. Environ. Eng.* **1997,** *123*, 371-380.

(5) Rosca, V.; Duca, M.; de Groot, M. T.; Koper, M. T. M., Nitrogen Cycle Electrocatalysis. *Chem. Rev.* **2009,** *109*, 2209-2244.

(6) Duca, M.; Koper, M. T. M., Powering Denitrification: the Perspectives of Electrocatalytic Nitrate Reduction. *Energy Environ. Sci.* **2012,** *5*, 9726-9742.

(7) Dima, G. E.; de Vooys, A. C. A.; Koper, M. T. M., Electrocatalytic Reduction of Nitrate at Low Concentration on Coinage and Transition-Metal Electrodes in Acid Solutions. *J. Electroanal. Chem.* **2003,** *554*, 15-23.

(8) Duca, M.; van der Klugt, B.; Koper, M. T. M., Electrocatalytic Reduction of Nitrite on Transition and Coinage Metals. *Electrochim. Acta* **2012,** *68*, 32-43.

(9) Rima, F. R.; Nakata, K.; Shimazu, K.; Osawa, M., Surface-Enhanced Infrared Absorption Spectroscopic Studies of Adsorbed Nitrate, Nitric Oxide, and Related Compounds. 3. Formation and Reduction of Adsorbed Nitrite at a Platinum Electrode. *J. Phys. Chem. C* **2010,** *114*, 6011-6018.

(10) Souza-Garcia, J.; Ticianelli, E. A.; Climent, V.; Feliu, J. M., Nitrate Reduction on Pt Single Crystals with Pd Multilayer. *Electrochim. Acta* **2009,** *54*, 2094-2101.

(11) de Vooys, A. C. A.; Koper, M. T. M.; van Santen, R. A.; van Veen, J. A. R., Mechanistic Study on the Electrocatalytic Reduction of Nitric Oxide on Transition-Metal Electrodes. *J. Catal.* **2001,** *202*, 387-394.

(12) de Vooys, A. C. A.; van Santen, R. A.; van Veen, J. A. R., Electrocatalytic Reduction of NO_3^- on Palladium/Copper Electrodes. *J. Mol. Catal. A: Chem.* **2000,** *154*, 203-215.

(13) Yang, J.; Duca, M.; Schouten, K. J. P.; Koper, M. T. M., Formation of Volatile Products during Nitrate Reduction on a Sn-modified Pt Electrode in Acid Solution. *J. Electroanal. Chem.* **2011,** *662*, 87–92.

(14) Taniguchi, I.; Nakashima, N.; Yasukouchi, K. Reduction of Nitrate to Give Hydroxylamine at a Mercury Electrode Using Cobalt(III)–and Nickel(II)–Cyclams as Catalysts. *J. Chem. Soc., Chem. Commun.* **1986**, 1814-1815.

(15) Shen, J.; Birdja, Y. Y.; Koper, M. T. M., Electrocatalytic Nitrate Reduction by a Cobalt Protoporphyrin Immobilized on a Pyrolytic Graphite Electrode. *Langmuir* **2015,** *31*, 8495-8501.

(16) Clayborne, A.; Chun, H. J.; Rankin, R. B.; Greeley, J., Elucidation of Pathways for NO Electroreduction on Pt(111) from First Principles. *Angew. Chem. Int. Ed.* **2015,** *54*, 8255-8258.

(17) de Vooys, A. C. A.; Beltramo, G. L.; van Riet, B.; van Veen, J. A. R.; Koper, M. T. M., Mechanisms of Electrochemical Reduction and Oxidation of Nitric Oxide. *Electrochim. Acta* **2004,** *49*, 1307-1314.

(18) de Vooys, A. C. A.; Koper, M. T. M.; van Santen, R. A.; van Veen, J. A. R., Mechanistic Study of the Nitric Oxide Reduction on a Polycrystalline Platinum Electrode. *Electrochim. Acta* **2001**, *46*, 923–930

(19) Duca, M.; Kavvadia, V.; Rodriguez, P.; Lai, S. C. S.; Hoogenboom, T.; Koper, M. T. M., New Insights into the Mechanism of Nitrite Reduction on a Platinum Electrode. *J. Electroanal. Chem.* **2010,** *649*, 59-68.

(20) Pletcher, D.; Poorabedi, Z., The Reduction of Nitrate at a Copper Cathode in Aqueous Acid. *Electrochim. Acta* **1979,** *24*, 1253-1256.

(21) Bae, S. E.; Stewart, K. L.; Gewirth, A. A., Nitrate Adsorption and Reduction on Cu(100) in Acidic Solution. *J. Am. Chem. Soc.* **2007,** *129*, 10171-10180.

(22) Bae, S. E.; Gewirth, A. A., Differential Reactivity of Cu(111) and Cu(100) during Nitrate Reduction in Acid Electrolyte. *Faraday Discuss.* **2008,** *140*, 113-123.

(23) Iwase, K.; Yoshioka, T.; Nakanishi, S.; Hashimoto, K.; Kamiya, K., Copper-Modified Covalent Triazine Frameworks as Non-Noble-Metal Electrocatalysts for Oxygen Reduction. *Angew. Chem. Int. Ed.* **2015**, *54*, 11068-11072.

(24) Kamiya, K.; Kamai, R.; Hashimoto, K.; Nakanishi, S., Platinum-Modified Covalent Triazine Frameworks Hybridized with Carbon Nanoparticles as Methanol-Tolerant Oxygen Reduction Electrocatalysts. *Nat. Commun.* **2014,** *5*, 5040.

(25) Kamiya, K.; Hashimoto, K.; Nakanishi, S., Graphene Defects as Active Catalytic Sites that are Superior to Platinum Catalysts in Electrochemical Nitrate Reduction. *ChemElectroChem* **2014,** *1*, 858-862.

(26) Ozaki, T., Variationally Optimized Atomic Orbitals for Large-Scale Electronic Structures. *Phys. Rev. B* **2003,** *67*, 155108.

(27) Ozaki, T.; Kino, H., Numerical Atomic Basis Orbitals from H to Kr. *Phys. Rev. B* **2004,** *69*, 195113.

(28) Lamy-Pitara, E.; El Mouahid, S.; Barbier, J., Effect of Anions on Catalytic and Electrocatalytic Hydrogenations and on the Electrocatalytic Oxidation and Evolution of Hydrogen on Platinum. *Electrochim. Acta* **2000,** *45*, 4299-4308.

(29) Wu, J. J.; Zhang, D.; Niwa, H.; Harada, Y.; Oshima, M.; Ofuchi, H.; Nabae, Y.; Okajima, T.; Ohsaka, T., Enhancement in Kinetics of the Oxygen Reduction Reaction on a Nitrogen-Doped Carbon Catalyst by Introduction of Iron via Electrochemical Methods. *Langmuir* **2015,** *31*, 5529-5536.

(30) Bogicevic, A.; Hass, K. C., NO Pairing and Transformation to N_2O on Cu(111) and Pt(111) from First Principles. *Surf. Sci.* **2002,** *506*, L237-L242.

(31) Padama, A. A. B.; Kishi, H.; Arevalo, R. L.; Moreno, J. L. V.; Kasai, H.; Taniguchi, M.; Uenishi, M.; Tanaka, H.; Nishihata, Y., NO Dissociation on Cu(111) and Cu_2O(111) Surfaces: a Density Functional Theory based Study. *J. Phys.: Condens. Matter.* **2012,** *24*, 175005.

(32) Yen, M. Y.; Ho, J. J., Density-Functional Study for the NOx (x=1, 2) Dissociation Mechanism on the Cu(111) Surface. *Chem. Phys.* **2010,** *373*, 300-306.

(33) Getman, R. B.; Schneider, W. F., DFT-based Characterization of the Multiple Adsorption Modes of Nitrogen Oxides on Pt(111). *J. Phys. Chem. C* **2007,** *111*, 389-397.

(34) Calle-Vallejo, F.; Huang, M.; Henry, J. B.; Koper, M. T. M.; Bandarenka, A. S., Theoretical Design and Experimental Implementation of Ag/Au Electrodes for the Electrochemical Reduction of Nitrate. *Phys. Chem. Chem. Phys.* **2013,** *15*, 3196-3202.

(35) Yang, J.; Calle-Vallejo, F.; Duca, M.; Koper, M. T. M., Electrocatalytic Reduction of Nitrate on a Pt Electrode Modified by p-Block Metal Adatoms in Acid Solution. *ChemCatChem.* **2013,** *5*, 1773-1783.

(36) Nijem, N.; Bluhm, H.; Ng, M. L.; Kunz, M.; Leone, S. R.; Gilles, M. K., Cu^{1+} in HKUST-1: Selective Gas Adsorption in the Presence of Water. *Chem. Commun.* **2014,** *50*, 10144-10147.

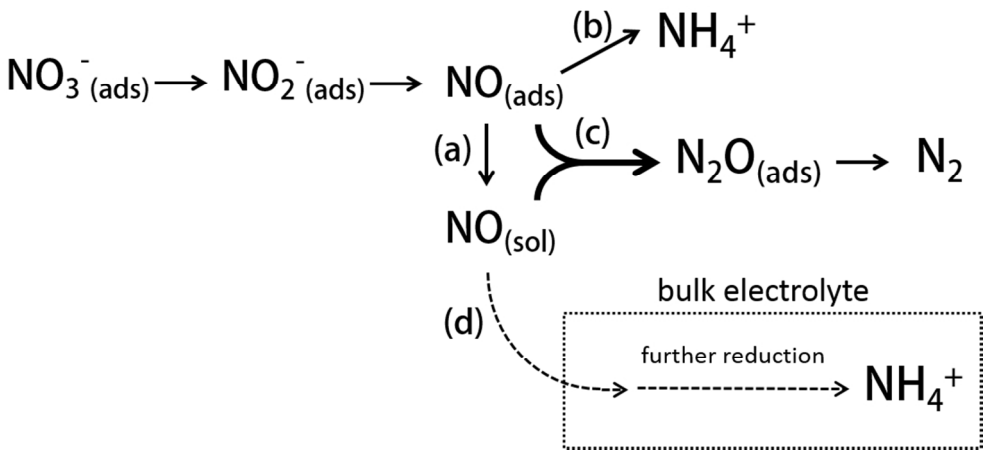

Scheme 1. Major reaction pathway for the electrochemical reduction of nitrate.
295x135mm (96 x 96 DPI)

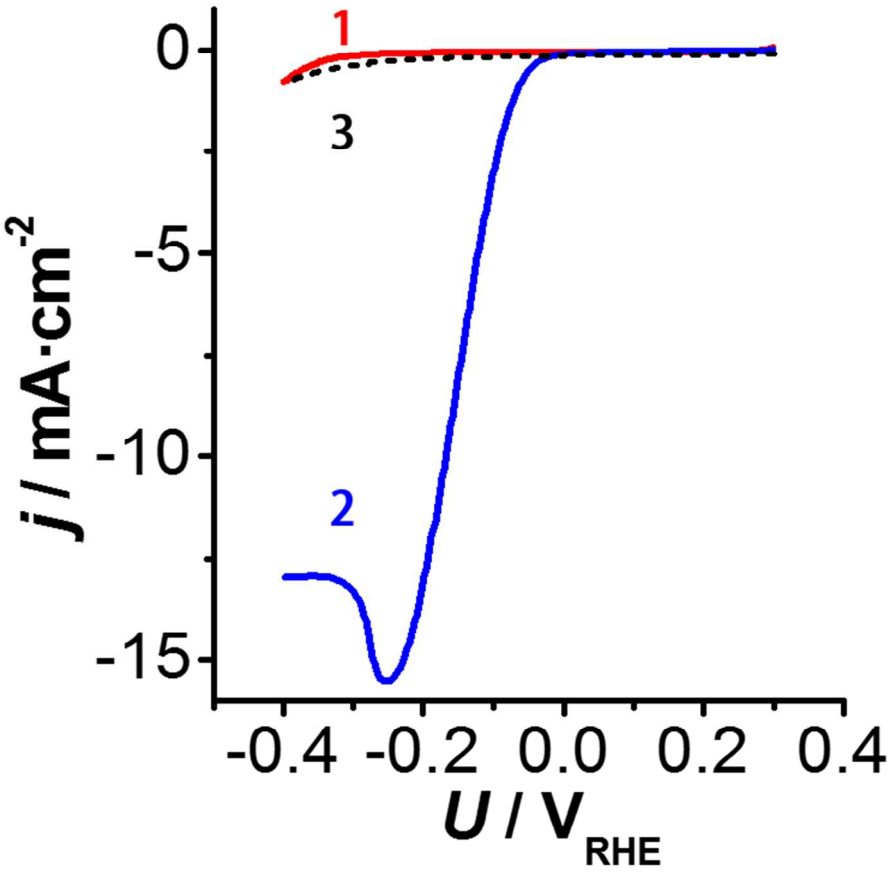

Figure 1. Current density (j) versus potential (U) curves for Cu-CTF in 0.1 M $HClO_4$ (curve 1, red) and 0.1 M $HClO_4$ + 0.1 M $NaNO_3$ (curve 2, blue), and for CTF (without Cu) in 0.1 M $HClO_4$ + 0.1 M $NaNO_3$ (curve 3, black, broken line).
220x213mm (96 x 96 DPI)

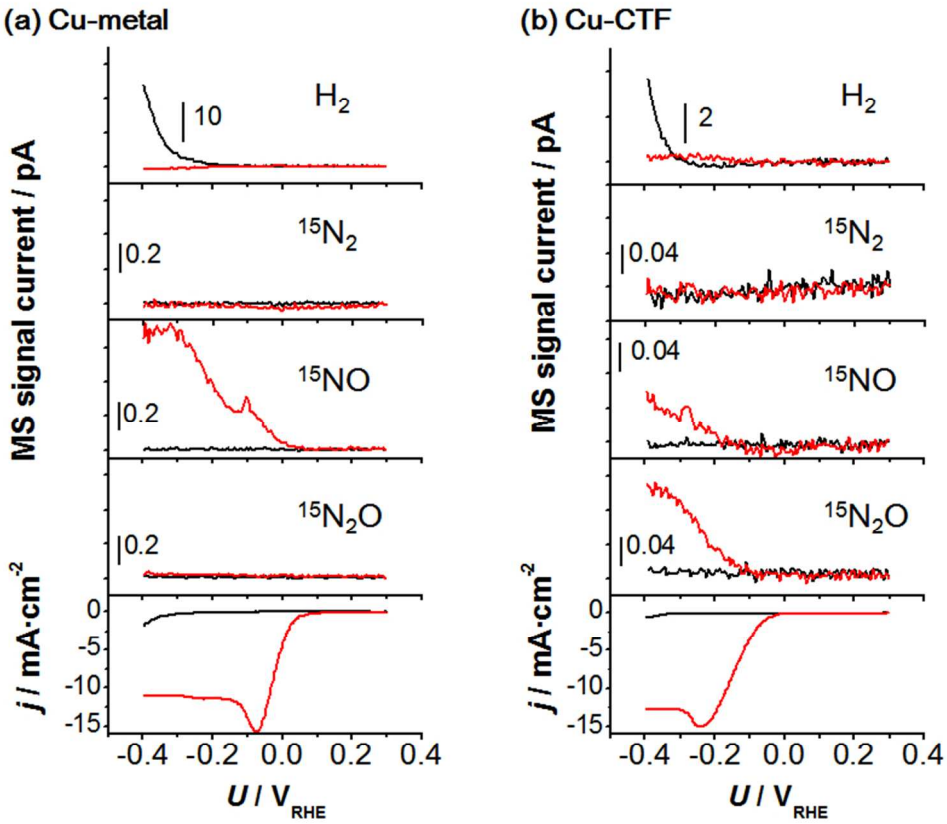

Figure 2. Mass signals assigned to H_2, $^{15}N_2$, ^{15}NO and $^{15}N_2O$, and the corresponding NRR currents for (a) Cu metal electrodes and (b) Cu-CTF in 0.1 M $HClO_4$ (black) or 0.1 M $HClO_4$ + 0.1 M $Na^{15}NO_3$ (red). The absolute value of the signals is dependent on the experimental conditions, particularly the distance between the electrode and detector, and the pressure in the mass spectrometer, which may have differed slightly between experiments.
219x187mm (96 x 96 DPI)

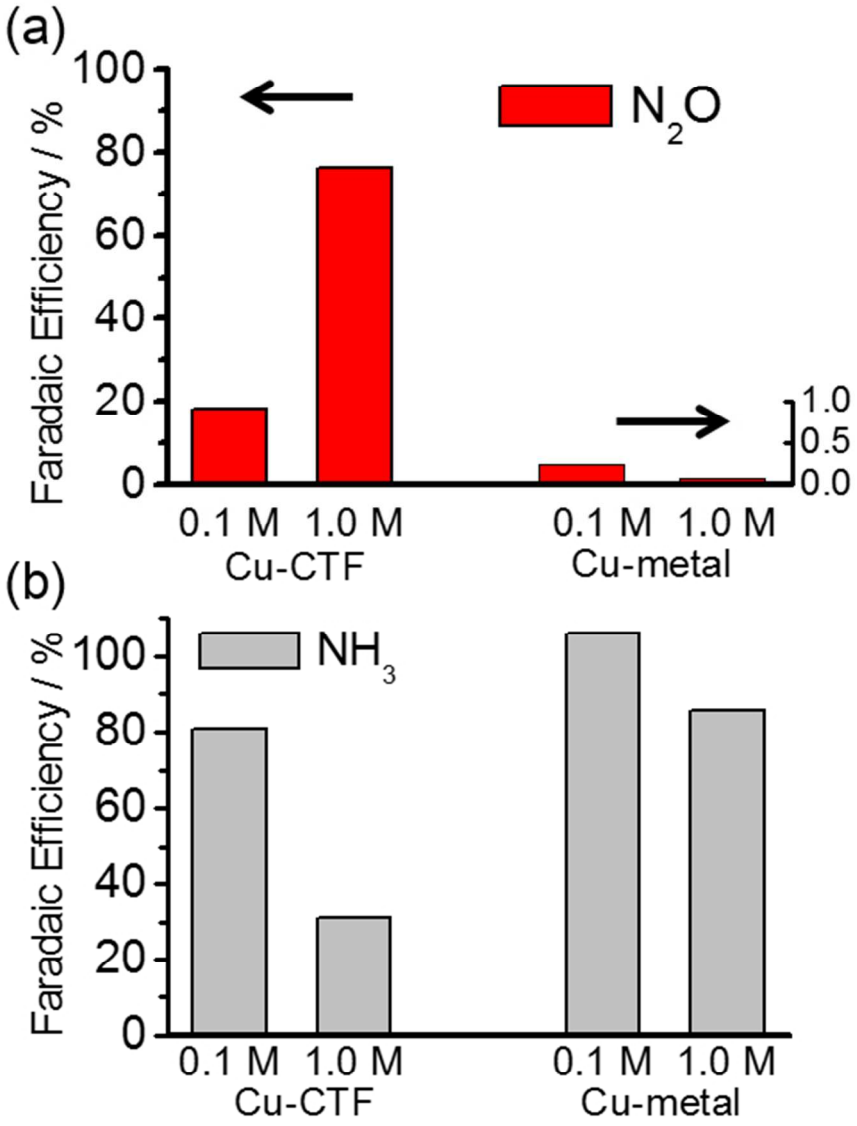

Figure 3. Faradaic efficiency for (a) N_2O and (b) NH_3 of Cu-CTF and Cu metal under a potentiostatic condition at - 0.2 V (vs RHE) for 60 min in 0.1 M $HClO_4$ + 0.1 M or 1.0 M $NaNO_3$. N_2, NO_2- and hydrogen were not detected. NO is not detectable by the GC-MS used in this study.
159x205mm (96 x 96 DPI)

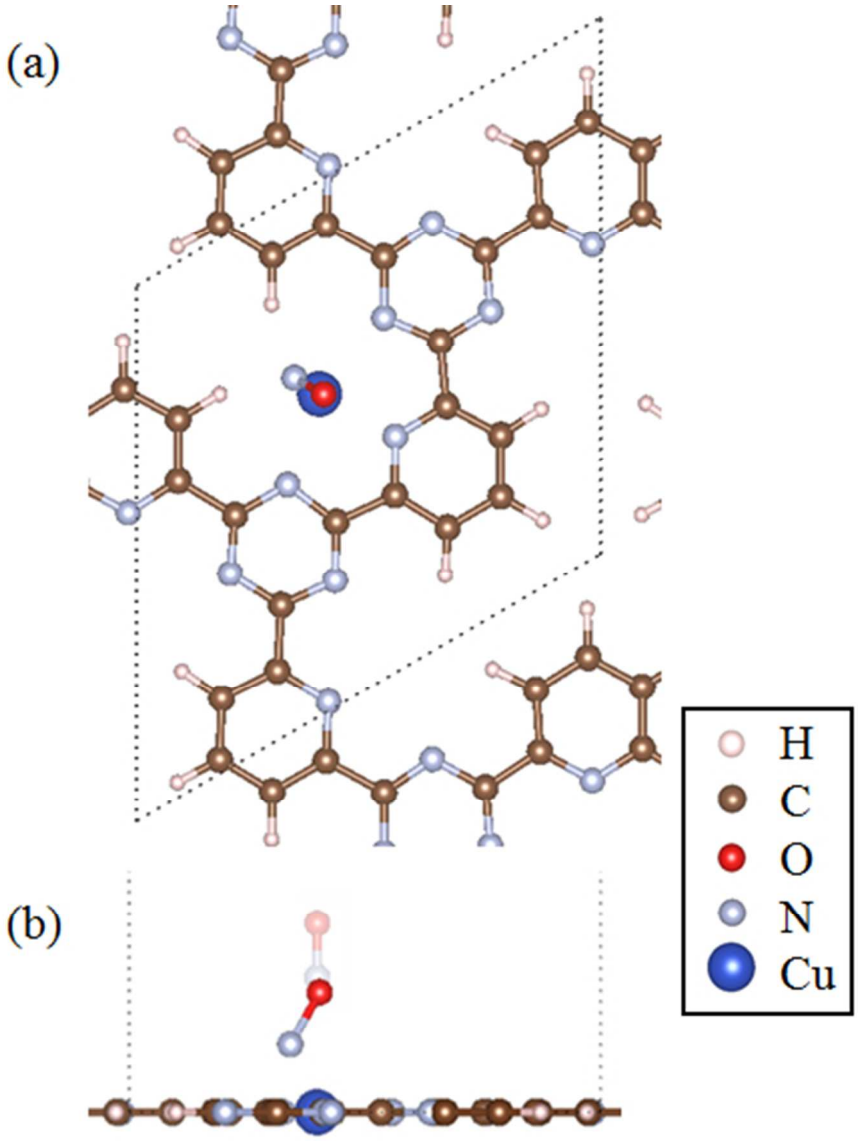

Figure 4. (a) Top and (b) side views of optimized structures of NO-adsorbed Cu-CTF. The initial position of NO is translucently displayed in (b).
117x150mm (96 x 96 DPI)

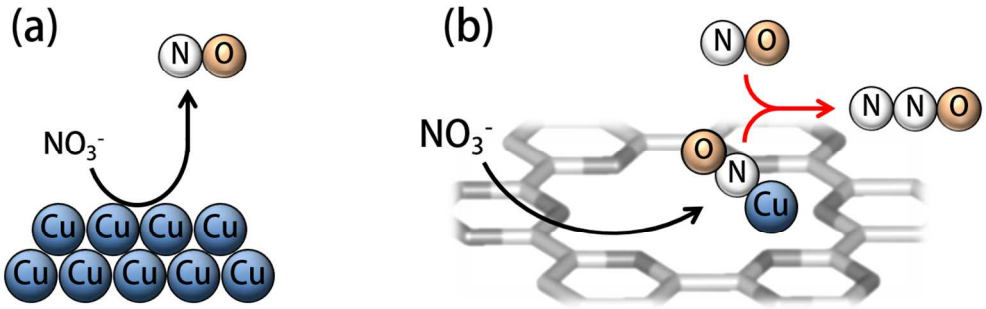

Figure 5. Schematic images of the reaction mechanism for N_2O formation on (a) Cu metal and (b) single-Cu-site catalyst (Cu-CTF).
365x118mm (96 x 96 DPI)

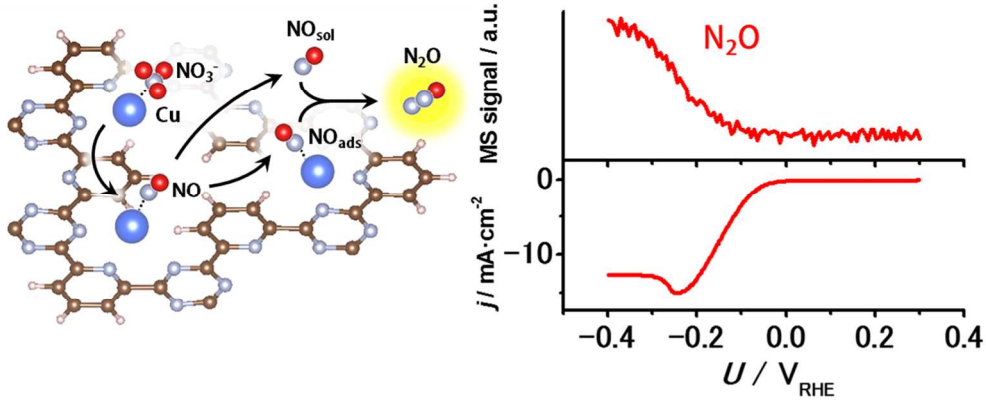

Table of Contents
328x137mm (96 x 96 DPI)